Available online at www.sciencedirect.com
SCIENCE DIRECT®
Acta Materialia 52 (2004) 573–581
Acta MATERIALIA
www.actamat-journals.com

Damage evolution of Nextel 610™ alumina fibre reinforced aluminium

B. Moser [a,b,*], A. Rossoll [a], L. Weber [a], O. Beffort [b], A. Mortensen [a]

[a] *Laboratory for Mechanical Metallurgy, Swiss Federal Institute of Technology EPFL, Lausanne, Switzerland*
[b] *Section Materials Technology, Swiss Federal Laboratories for Materials Testing and Research EMPA, Thun, Switzerland*

Received 15 December 2002; received in revised form 26 September 2003; accepted 27 September 2003

Abstract

It is shown that tensile testing of continuous fibre reinforced composite specimens with varying gauge lengths above the matrix melting temperature provides a method for the measurement of fibre damage within the composite. This method is applied to a composite wire of alumina fibres reinforcing a pure Al or an Al–2%Cu matrix. It is found that the wire contains a finite initial level of fibre damage. Fibre damage accumulation caused by composite tensile straining is also measured by applying the method to previously stressed wire samples. The rate of damage accumulation for a single phase matrix composite is well described by the Weibull parameters of the virgin fibre, indicating that fibre strength is unaffected by composite processing. The presence of brittle second phases in the matrix increases, however, the rate of damage accumulation as compared to the rate expected from single fibre Weibull statistics.

Keywords: Tension test; Metal matrix composites; Aluminium; Fracture; Fibre breakage

1. Introduction

Continuous fibre reinforced aluminium is a type of composite with unique properties and application potential; yet, it is presently not entirely clear how such composites fail in tension, nor what constitutes a "good" metal matrix for these materials [1–4]. Contradictory data and interpretations exist concerning such fundamental issues as, for example, the extent to which load sharing around fibre breaks is global or local, the role played by the matrix in determining the strength of the composite, or the necessity of having weak, easily debonding fibre/matrix interfaces versus the strong interfaces generally observed in systems such as alumina fibre reinforced aluminium (e.g. [5,6]).

It is known that fibre breakage is the dominant damage mode in such composites, and that it clearly plays a key role in the succession of events leading to their tensile failure. The formation of isolated fibre breaks prior to tensile failure of fibre reinforced aluminium is well documented (e.g. [7]). Several techniques are presently used to measure the evolution of the fraction of broken fibres with axial stress.

Metallography is a simple method for detecting broken fibres [8,9]; however, the actual volume of fibres (total fibre length) sampled is usually small and possible artefacts due to fibre breakage during metallographic preparation are difficult to exclude [10,11]. In situ mechanical tests [12] under an optical or electronic microscope suffer from the same problem of small sampled fibre length, compounded by the fact that the fracture behaviour of fibres situated along the sample surface, which furthermore are often ablated during prior sample polishing, is likely to differ from that of fibres in the composite bulk.

Acoustic emission techniques have often been used to measure the damage evolution in fibre reinforced

* Corresponding author. Present address: Suresh Group, DMSE, Massachusetts Institute of Technology, 77 Massachusetts Avenue, Room 8-139, Cambridge, MA 02139, USA. Tel.: +1-617-2539825; fax: +1-617-2580390.
E-mail address: benedikt.moser@alumni.ethz.ch (B. Moser).

1359-6454/$30.00 © 2003 Acta Materialia Inc. Published by Elsevier Ltd. All rights reserved.
doi:10.1016/j.actamat.2003.09.040

composite materials and structures [7,13–18]. These investigations confirm the presence of progressive fibre fracture prior to final composite failure. Quantitative interpretation of the results (e.g. in terms of number of fibre breaks as a function of applied stress) was successfully done for monofilament reinforced metals; however, with fibres typically used for reinforcing aluminium (fibre diameter on the order of 10 μm, versus about 100 μm for monofilaments) the energy release due to a single fibre break is much smaller. This makes a quantitative interpretation of such data difficult [16].

More indirect measurements of the presence of fibre breaks, such as monitoring the evolution of the composite longitudinal Young's modulus, have also been used to assess damage, e.g. in alumina fibre reinforced magnesium subjected to thermomechanical fatigue [19]. This method is made difficult by several complicating effects, such as effects of non-linear elasticity in the reinforcing fibres, the importance of which was recently brought to light for such composites in [20]. Density variations as a measure of damage have also been investigated. In [19] a density decrease after thermomechanical cycling was detected but mainly attributed to the formation of microvoids at the fibre-matrix interface and in the matrix rather than to fibre breaks.

A new method for the measurement of internal damage over comparatively large composite volumes is presented in this paper. The method consists of conducting tensile tests on long metal matrix composite specimens while the gauge length is held at a temperature above the melting point of the matrix. The measured composite strength at this temperature can be quantitatively related to the density of fibre breaks present in the composite. With the application of prior deformation on the composites in the solid state, this technique allows the measurement of damage evolution in the composites prior to failure, which in turn can be used to gain insight into the process that leads to final composite tensile failure.

The method is applied to measure the damage evolution in two alumina fibre reinforced aluminium composites, namely Nextel 610^{TM}/Al and Nextel 610^{TM}/Al–2%Cu. The experimental results presented are confronted with the damage evolution expected according to a two-parameter Weibull distribution that is most commonly used to describe failure of brittle fibres [21].

2. Experimental procedures

2.1. Materials

Two continuous alumina fibre reinforced aluminium matrix composite wires are investigated in this study. The wires are produced by 3M (St. Paul, MN, USA) and supplied on a reel. The reinforcement of the wire consists in about 50 vol% of the continuous alumina fibre Nextel 610^{TM} (3M, St. Paul, MN, USA). The main fibre properties are summarized in Table 1; more detailed data can be found in [22–24]. The wire is produced by an ultrasound-driven liquid metal infiltration technique [25]. The final wire has a roughly circular cross-section with an equivalent diameter of 1.99 mm (determined by volume measurement). Pure Al (>99.98%) and Al–2%Cu are used as matrix materials. The Al–2%Cu matrix wire is investigated in the as-cast as well as in the solutionized condition (16 h at 520 °C in air, followed by a water quench). Due to limitations in the length of available furnaces, wires with a gauge length longer than 230 mm were not tested in the heat-treated condition.

2.2. Microstructure

The microstructure of the composites was investigated by optical and scanning electron microscopy. Additionally, the wire material was characterized by a transmitted light microscopy (TLM) technique, the details of which are described elsewhere [26].

2.3. Damage measurement

To measure fibre damage within the composites, tensile tests were conducted while a selected length of the wire between the grips was kept at a constant temperature of 775 °C using custom-built resistance tube furnaces with an inner tube diameter of 5 mm (the data interpretation methodology is explained below). All tensile tests were performed using an Alliance RT/50 (MTS, MN, USA) computer-controlled tensile testing machine equipped with a 5 kN load cell. The specimen was gripped using either mechanical or hydraulic grips. The molten length of the wire was changed by varying the number of heated zones or by varying the length of the furnace. The length of the molten composite wire zone l was measured by subtracting the length of the non-molten part of the wire (measured after the test) from the initial wire length (measured before testing); the non-molten part is assumed to undergo only

Table 1
Main properties of the Nextel 610^{TM} alumina fibre

Composition [22]	>99% α-Al_2O_3
	0.2–0.3%SiO_2
	0.4–0.7%Fe_2O_3
Mean UTS at $L_0 = 25.4$ mm [23,24]	3.3–3.47 GPa
Weibull modulus [23]	9.7–11.2
Young's modulus [23]	373 GPa
Density [22,23]	3.75–3.9 g cm^{-3}
Diameter [23]	11.98 μm
CTE (100–1100 °C) [37]	8×10^{-6} K^{-1}

negligible irreversible deformation during the test. The molten and non-molten parts of the wire were easily distinguished after the test by their different levels of surface tarnish. The tests were conducted under constant crosshead displacement speed between 10 and 200 μm/s depending on the molten length, corresponding to a strain rate of roughly 5×10^{-4} s^{-1}. The maximum stress is calculated from the maximum load divided by the average initial wire cross-section before melting. Some of the specimens underwent a prestressing load cycle at room temperature by applying an axial tensile stress, σ_{pre}, to the composite of between 1000 and 1300 MPa followed by unloading, before testing at 775 °C.

3. Results

3.1. Microstructure

3.1.1. Fibre distribution and volume fraction

The composite wire shows a characteristic "S"-shape fibre distribution with some regions of lower fibre volume fraction, Fig. 1. This is related to the processing, indicating that a flat fibre bundle was folded to form the round wire: the low volume fraction regions in the wire correspond to the space between two surfaces of the formerly flat fibre bundle [27]. The average wire fibre volume fraction was determined by densitometry to be roughly 50 vol%.

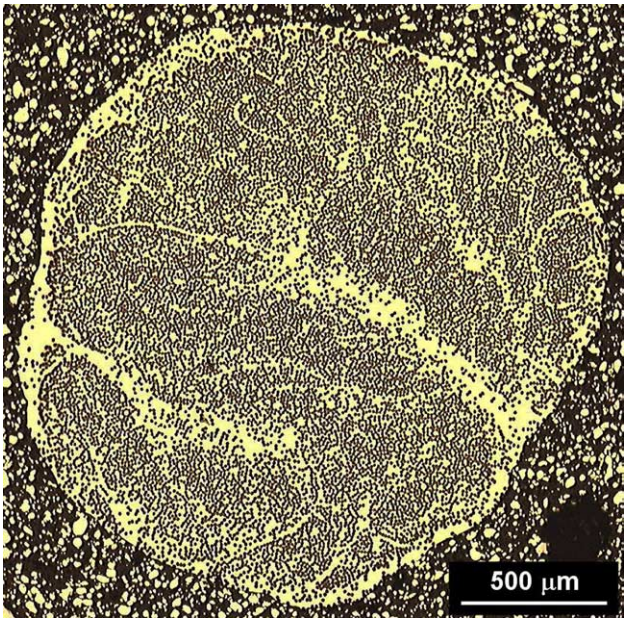

Fig. 1. Optical micrograph of the cross-section of the continuous alumina fibre reinforced composite wire. The folded fibre tows are clearly visible (the folds can be distinguished by the two fibre-free matrix regions roughly one wire radius deep).

3.1.2. Al–2%Cu matrix microstructure

The composite wire with the binary Al–2%Cu matrix in the as-cast condition contains a considerable amount of copper-rich second phases. These are composed primarily of Al_2Cu θ-phase according to the binary phase diagram (other Al–Cu intermetallics are also present due to impurities such as iron) [28]. Copper-rich second phases are preferentially located along the fibre-matrix interface and in regions where two or more fibres are in close contact, Fig. 2(a). Solutionizing at 520 °C for 16 h in air followed by water quenching dissolves most of these intermetallics; however, there are still some residual intermetallics present at contact points between two fibres, Fig. 2(b).

3.2. Composite strength with a molten matrix (at 775 °C)

The tensile strength of the pure Al/Nextel 610™ composite wire at 775 °C is shown in Fig. 3 (filled black circles). A clear decrease in strength with increasing molten wire length is visible. It follows additionally from Fig. 3 that prestressing the wire at room temperature before melting leads to a further decrease in strength (open squares, triangles and circles).

Figs. 4 and 5 show the strength of the Al–2%Cu/Nextel 610™ composite wire at 775 °C, in the as-cast and the solutionized condition, respectively (filled black circles). The strength decrease with increasing molten length l in the as-cast condition, Fig. 4 (filled black circles), is roughly the same as for the pure Al matrix composite. The strength at shorter molten lengths is somewhat lower. The effect of prestressing, however, is much greater for the alloyed matrix in the as-cast condition than for the pure Al matrix composite, Fig. 4 (open rhombi and squares).

After solutionizing, Fig. 5 (filled black circles), the strength of the alloyed wire at shorter molten length is higher again and reaches almost that of the pure aluminium matrix wire. The effect of prestressing, Fig. 5 (open triangles and circles), is similar to that found in the pure aluminium matrix composite.

The composite fracture behaviour changes gradually from abrupt fracture at shorter molten zone lengths to a smooth load decrease after reaching maximum load at longer molten zone lengths, see Fig. 6. For specimens with a molten length l below 50 mm, macroscopic failure of the specimen was usually observed at the solid/liquid transition, Fig. 7 (left). For $l \geqslant 50$ mm, Fig. 7 (right), no macroscopic specimen separation was observed and the stress decreased smoothly after its peak value to a finite remanent value after failure, Fig. 6. This value varied roughly proportionally with l, reaching 40 MPa with a molten length of 507 mm, but was not significantly affected by the crosshead displacement rate.

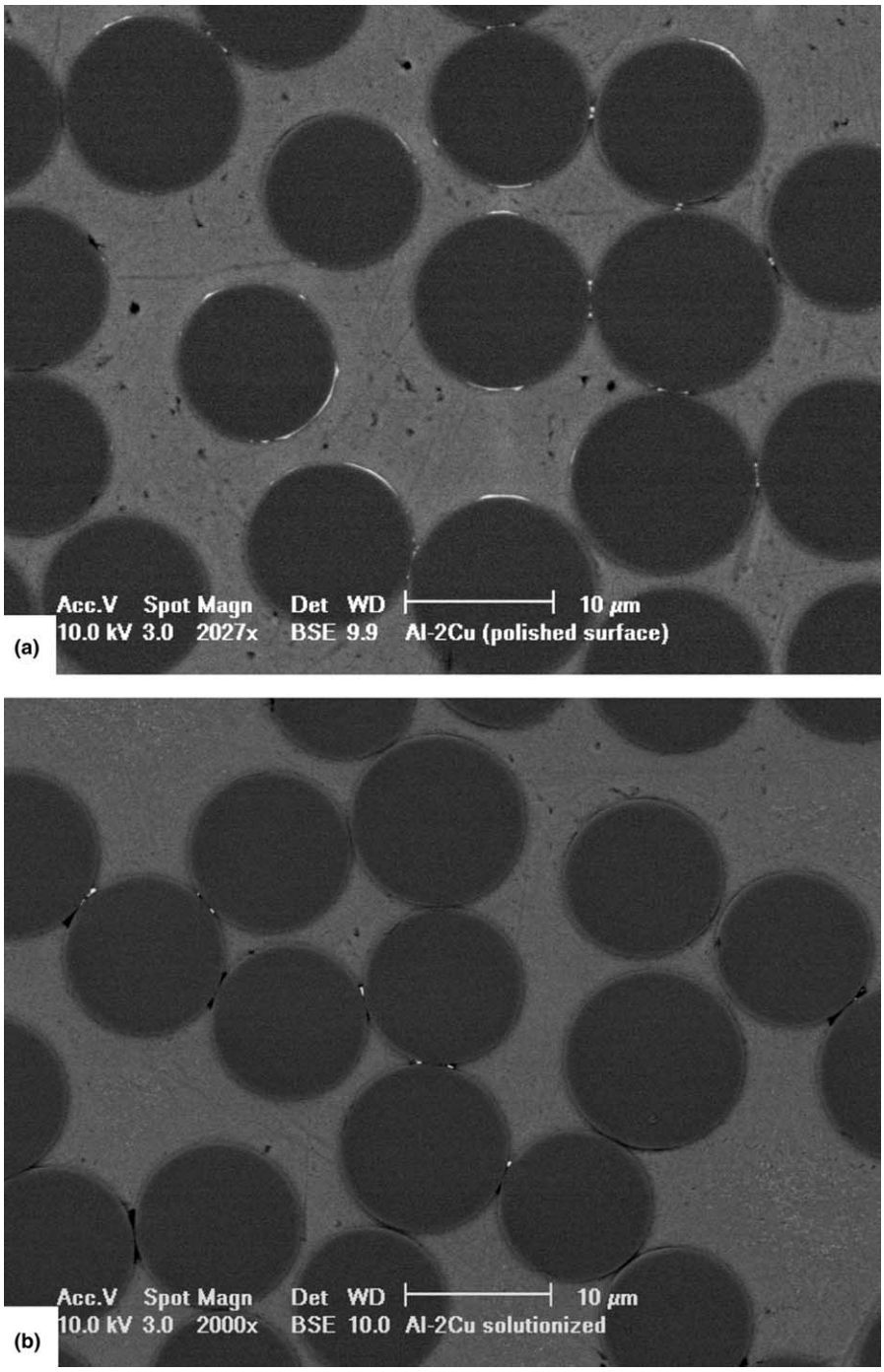

Fig. 2. Backscattered electron micrograph (BSE) of a metallographically polished cross-section of the Al–2%Cu/Nextel 610^{TM} composite wire in the (a) as-cast condition and (b) after heat treatment (solutionizing at 520 °C for 16 h and quenched in water). In the as-cast condition (a), the Al_2Cu intermetallics are clearly visible as white regions around some of the fibres. Some residual second-phases are still visible at contact points between two fibres after solutionizing (b).

4. Discussion

4.1. Initial damage

4.1.1. Pure Al matrix composite wire

It was observed in tensile testing of molten wires with shorter lengths ($l < 50$ mm) that:

(i) fracture of the wire (i.e. of the fibres in molten aluminium) occurred invariably at the solid/liquid transition, Fig. 7 (left), and
(ii) the measured wire strength at $l = 20$ mm (~650 MPa) is significantly lower than the expected fibre bundle strength for this length, corrected for the fibre volume fraction (~1300 MPa) [29,30].

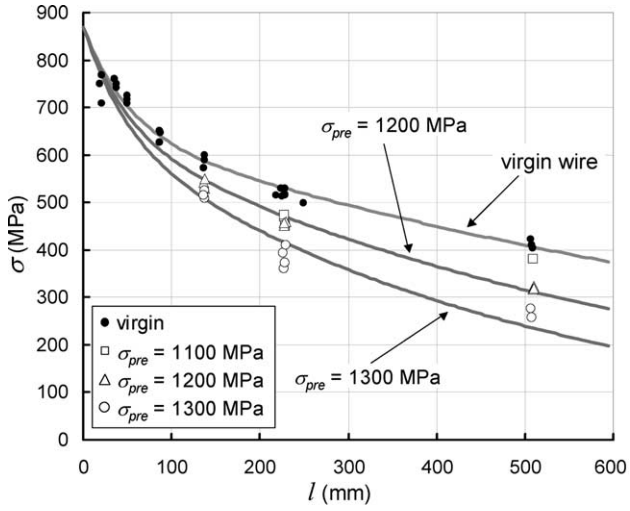

Fig. 3. Strength of the pure Al matrix composite wire at 775 °C as a function of the molten length and the prestress level. The continuous lines are manual fits according to Eq. (3) with parameters given in the text, Section 4.1.1 (top curve) and 4.2.1 (lower two curves).

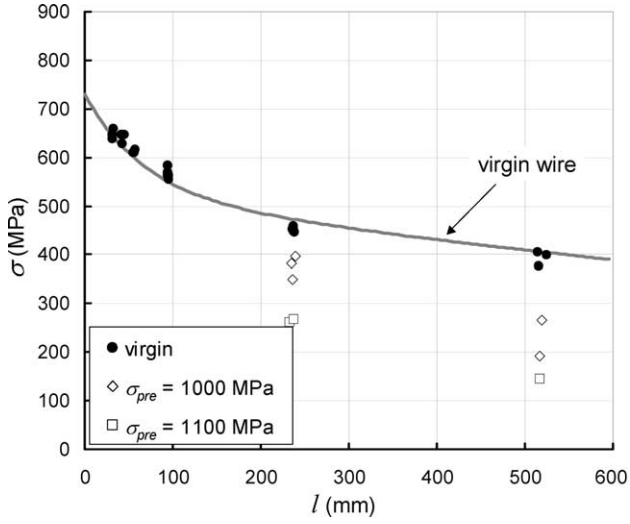

Fig. 4. Strength of the Al–2%Cu matrix composite wire at 775 °C as a function of the molten length and the prestress level in the as-cast condition. The prestressing as well as the subsequent testing at 775 °C were carried out with the wire in the as-cast condition. The continuous line is a manual fit according to Eq. (3) with parameters given in the text, Section 4.1. Compare the effect of prestressing with Fig. 3 to see that damage is much higher for the Al–2%Cu matrix in the as-cast condition.

A plausible explanation for these observations is that, at the solid/liquid matrix interface stress concentrations act on the fibres, in all likelihood because fibres that emerge from the aluminium solid/liquid interface experience stress concentrations due to bending whenever their axis is not strictly parallel to the stress axis. This stress concentration, in turn, results in localized fracture of stressed fibres at the solid/liquid interface, at a stress

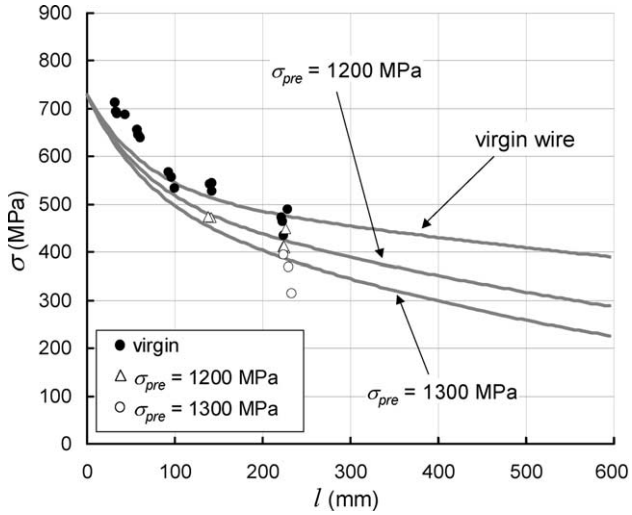

Fig. 5. Strength of the Al–2%Cu matrix composite wire at 775 °C as a function of the molten length and the prestress level. The prestressing as well as the subsequent testing at 775 °C were carried out after solutionizing the wire at 520 °C in air for 16 h followed by water quenching. The top continuous line is the manual fit according to Eq. (3) drawn with the same parameters used for the as-cast wire in Fig. 4. The lower two lines are drawn with calculated parameters under the assumption that damage accumulates with the same rate as in the case of the pure aluminium matrix wire. The parameters are $C = 730$ MPa, $c_1 = 0.28$, $D_1^{\sigma_{pre}} = 0.0155$, and $D_2^{\sigma_{pre}} = 1.01 \times 10^{-3}$ for a prestress of 1200 MPa and $C = 730$ MPa, $c_1 = 0.28$, $D_1^{\sigma_{pre}} = 0.0159$, and $D_2^{\sigma_{pre}} = 1.418 \times 10^{-3}$ for a prestress of 1300 MPa, for a reference length of 1 mm.

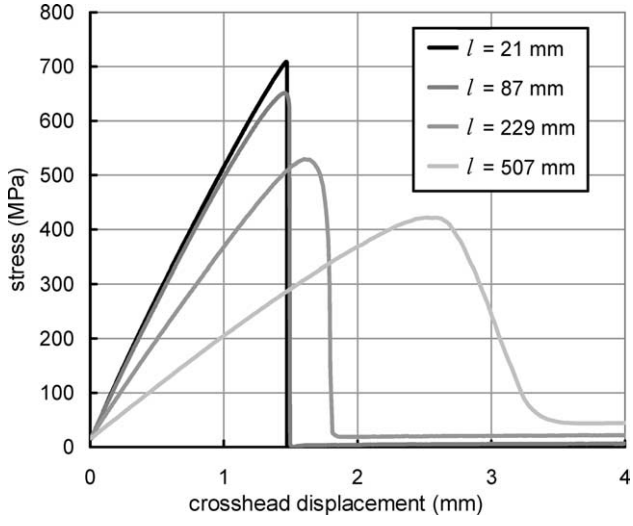

Fig. 6. Plots of stress–displacement curves showing the difference in fracture behaviour found on varying the molten length l.

significantly lower than the nominal average fibre fracture stress.

As the molten wire segment length is increased, the macroscopically observed fibre fracture becomes increasingly less concentrated at the solid/liquid matrix interface. Many fibres still break there (Fig. 7); however,

Fig. 7. Left: macroscopic failure at the solid/liquid transition for specimens with a molten length $l \leqslant 50$ mm. Right: two specimens with $l > 50$ mm after failure (i.e. strained beyond the peak stress); the lower specimen is as-retrieved from the tensile testing apparatus, the upper specimen was pulled apart while molten until full separation in two halves.

an increasing fraction of fibres has already fractured elsewhere, within the molten zone, from which they pull out gradually after the composite reaches its peak stress. This is consistent with the observation of a finite friction stress after failure, most likely caused by fibres rubbing one against the other under the action of capillary forces (which have been shown to be substantial for fibres 8 μm in diameter [31]). This explanation is also consistent with the observation that this remanent stress increases roughly in proportion with l, Fig. 6.

Additionally, the wire tensile strength decreases as the molten zone length increases: there is thus a size effect. A size effect is expected if the fibres in the molten portion of the wire behave like a dry fibre bundle. Two-parameter Weibull statistics describes the behaviour of such a dry fibre bundle and the survival probability S_{Weibull} of a fibre under an axial stress of σ_f is a function of its length L and of its Weibull parameters (characteristic strength σ_0 at length L_0 and Weibull modulus m)

$$S_{\text{Weibull}} = \exp\left[-\frac{L}{L_0}\cdot\left(\frac{\sigma_f}{\sigma_0}\right)^m\right]. \quad (1)$$

The size effect for the strength of the dry fibre bundle expected from the literature parameters (Table 1) and the experimentally measured size effect on the molten wire length l (both normalized with strength at $L = l = 20$ mm) are plotted together in Fig. 8. It is seen that the molten wire strength exhibits a significantly greater size effect than expected for the dry fibre bundle. Since the fibres are known to be inert in molten aluminium, it is highly unlikely that their strength would be degraded by the presence of the molten matrix. Hence, it is concluded that the fibres in the composite wire were already damaged before testing, most likely during processing of the wire.

The presence and nature of such damage are confirmed by TLM [26]. This method quantifies the amount of damage present in the form of "dead" fibre ends

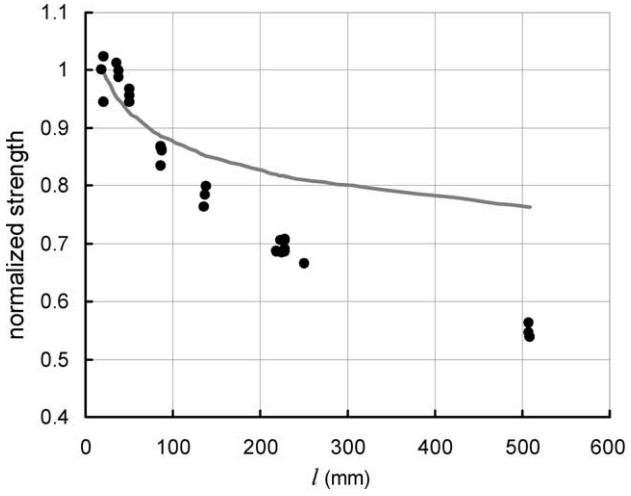

Fig. 8. The size effect as observed in the molten wire experiment (filled black circles) for the pure aluminium matrix composite and as expected by the two-parameter fibre Weibull distribution (grey solid line). The strength is normalized for a length of the specimen or of the molten zone of 20 mm, respectively.

within the wire, i.e., fibres that terminate within the matrix. Such fibre ends can be explained either by the presence of ending fibres in the initial fibre tows, or by fibre fracture followed by relative displacement of the fractured fibre ends during wire processing prior to matrix solidification. Since fractured or terminating fibres can clearly not carry load within the molten zone (apart from a small amount due to friction) and since the number of fractured or terminating fibres increases linearly with the molten zone length, both the strength of the partially molten wire and the proportion of fibres breaking at the solid/liquid interface should decrease with increasing molten segment length, as observed.

After the peak load is passed, the remanent wire strength does not exceed 10% of the peak load. Hence, for the sake of simplicity, friction loads exerted by

broken fibres within the molten composite are neglected. The fracture load of the molten wire can then be calculated based on the following two assumptions:

(i) all fibres that end within the molten part do not carry any load and
(ii) fibres that are continuous throughout the molten part break at the solid/liquid transition, at an average stress value that is independent of the molten length (and is governed by the stress concentration at that location).

Under these assumptions, the composite fracture strength is simply proportional to the number of intact continuous fibres bridging the entire molten region (in the following called "surviving fibres"). This number is governed by pre-existing damage in the wire.

If the damage parameter D denotes the probability that a given fibre one millimetre long ends or is fractured within this length in the undeformed composite, the survival probability S (i.e. the probability that a fibre is intact) over length l, expressed in mm, can readily be calculated from the inverse probability $1 - D$ and equals $S = (1 - D)^{l/l_0}$, with $l_0 = 1$ mm as reference length.

Assuming that the number of surviving fibres is sufficiently large for the bundle strength to be governed by the asymptotic bundle strength [29], the fracture strength σ of a composite wire containing a molten region of length l can be written as

$$\sigma = C \cdot (1 - D)^{l/l_0}, \tag{2}$$

where C is the wire fracture stress at the solid/liquid interface for the limiting case where all fibres are intact (molten length $l = 0$ mm), equal to the bundle strength of the fibres at the solid/liquid matrix interface. According to Eq. (2) a plot of ln σ versus l should yield a straight line. It is found that this is not the case: the relation between the logarithmic strength of the composite and l is much closer to a bilinear correlation.

This can be rationalized by an additional observation from the TLM investigation of fibre damage in the wire [26]: close examination of TLM micrographs shows that most defective fibres are located either at the periphery of the wire, or along one of the two folds, visible as essentially fibre-free matrix regions. In other words, fibre damage is more extensive along the surface of the formerly flat fibre bundle, and less extensive inside this bundle. Ending fibres in the wire thus originate largely from surface damage of the fibre tows and the molten matrix composite wire during spooling and handling operations in the composite wire production process. A bimodal damage distribution is thus suggested by metallographic observation. If we separate the fibres into two populations with distinct damage parameters, corresponding respectively to the more damaged peripheral fibres and to less-damaged fibres within the tows, Eq. (2) is modified to

$$\sigma = C \cdot \left(c_1 \cdot (1 - D_1)^{l/l_0} + c_2 \cdot (1 - D_2)^{l/l_0}\right), \tag{3}$$

where subscripts 1 and 2 denote the two different fibre regions (formerly flat fibre bundle periphery and interior, respectively) and c_1 and c_2 their respective fractions ($c_1 + c_2 = 1$). The length l is as before counted in mm, and the two damage constants D_1 and D_2 are normalized to a length of one millimeter. As shown in Fig. 3, a good description of the experimental values of the pure aluminium matrix wire strength as a function of the molten zone length l is obtained using the following parameters (determined by a manual fit): $C = 870$ MPa, $c_1 = 0.25$, $D_1^{\text{virgin}} = 0.02$, $D_2^{\text{virgin}} = 9.3 \times 10^{-4}$. These parameters correspond to an average damage parameter (calculated by a rule of mixtures) of 5.7×10^{-3} for a length of 1 mm. This is close, but not quite equal to, the average damage parameter measured by TLM ($D = 6.8 \times 10^{-3}$ for 1 mm) [26]. The slight difference between results from the TLM study in [26] and the present experiments is most likely related to spool-to-spool variations [32].

4.1.2. Al–2%Cu matrix composite wire

The Al–2%Cu matrix composite wire exhibits a behaviour similar to that of the pure Al matrix composite. The wire strength at short molten length is lower in the as-cast Al–2%Cu wire than with the pure Al matrix. After the wire is solutionized the strength values approach almost the values measured for the pure Al matrix composites. Again the wire strength dependence on the length of the molten zone, l, can be described by a bimodal damage distribution with only slightly changed parameters compared to the pure aluminium matrix composite. The parameters for the as-cast Al–2%Cu matrix wire are $C = 730$ MPa, $c_1 = 0.28$, $D_1^{\text{virgin}} = 0.015$, $D_1^{\text{virgin}} = 5.0 \times 10^{-4}$, still for a reference length of 1 mm (top curve in Fig. 4). The resulting average damage parameter is 4.56×10^{-3} mm^{-1}. It is likely that the slightly lower value of C reflects a difference in the solid/liquid interface morphology (and hence in the resulting stress concentration factor on the fibres), while differences in damage distribution parameters probably reflect spool-to-spool variations noted previously, rather than an influence of the matrix.

4.2. Damage accumulation during deformation

4.2.1. Pure Al matrix composite wire

As shown above, testing locally molten wires provides a method of quantifying the level of fibre damage in the composite. Whether damage is present in the form of isolated fibre ends or broken fibres (two opposite fibre ends close together) does obviously not change the effect. Hence the method can be used to measure the amount of additional damage introduced in the

composite after it has been subjected in the solid state to a given applied stress σ_{pre}.

It is indeed found that prestressing in the solid state lowers the ultimate tensile strength of the partially molten wire at 775 °C, Fig. 3. As can be expected, the strength difference between prestressed and virgin composites also decreases as l decreases. Since scatter in the wire strength was found to increase as the molten zone length decreases, molten wire strength measurements for the prestressed wires were only conducted for $l > 100$ mm. The model presented above to describe the in situ fibre bundle strength as a function of fibre damage can now be used to describe the behaviour of the prestressed and hence damaged composite. To this end, only one parameter (damage parameter D_2) is changed independently to describe the experimental values of the prestressed composites, while the ratio between $(1 - D_1)$ and $(1 - D_2)$ and also the respective concentrations c_1 and c_2 as well as C are kept constant, on the reasoning that damage accumulates identically in intact fibres regardless of which region of the initial wire they belong to. This is justified as long as the average intact length is significantly longer than the critical shear length. The result of the manual fitting process is shown in Fig. 3: as seen it agrees quite well with the data. The parameters resulting from this fit are $C = 870$ MPa, $c_1 = 0.25$, $D_1^{\sigma_{pre}} = 0.0205$ and $D_1^{\sigma_{pre}} = 1.45 \times 10^{-3}$ for a prestress of 1200 MPa, and $C = 870$ MPa, $c_1 = 0.25, D_1^{\sigma_{pre}} = 0.0209$, and $D_2^{\sigma_{pre}} = 2.00 \times 10^{-3}$ for a prestress of 1300 MPa, always with a reference length of 1 mm.

This evolution of damage with prestress in the wire can be confronted with that expected from the intrinsic fibre strength Weibull distribution. The increase in damage created by prestressing (left-hand side of Eq. (4) below) should follow directly from the two parameter Weibull strength distribution of the Nextel 610™ fibres (right-hand side of Eq. (4)) for a fibre length of $L = 1$ mm (as the damage parameters are normalized for 1 mm)

$$\frac{1 - D_x^{\sigma_{pre}}}{1 - D_x^{virgin}} = S_{Weibull} = \exp\left[-\frac{L}{L_0} \cdot \left(\frac{\sigma_f}{\sigma_0} \right)^m \right], \qquad (4)$$

where x can be either 1 or 2. Using $m = 11.2$ and $\sigma_0 = 3.47$ GPa for $L_0 = 25.4$ mm (literature values from single fibre tests, see Table 1), the failure probabilities of a fibre of length $L = 1$ mm are 6.334×10^{-4} and 1.552×10^{-3}, for fibre stress levels σ_f of 2400 and 2600 MPa, respectively. These values are in fairly good agreement with the parameters used to describe the experimental data from the presented molten wire tests (Fig. 3), which lead to failure probabilities of 5.2×10^{-4} and 1.1×10^{-3}, respectively.

This result implies that the fracture of fibres in the solid matrix wire is mostly uncorrelated up to composite stresses of 1300 MPa (corresponding to a fibre stress of ~2600 MPa), which is about 93% of the composite tensile strength [32]. Indeed, the data from the single fibre tests are coherent with those from the tests on the composite with molten matrix.

4.2.2. Al–2%Cu matrix composite wire

Applying the same reasoning to the Al–2%Cu matrix wire, one observes that the same conclusion holds for the solutionized Al–2%Cu matrix as for the pure Al matrix composite: the progression of fibre fracture after deformation is comparable to that found in the pure aluminium matrix wire and therefore as expected from Weibull statistics of the virgin fibre (see Fig. 5 and compare with Fig. 3). Hence, it can be concluded that the fracture behaviour of the fibres is not per se affected by the presence of Cu dissolved in the matrix. This is as expected, given the fact that neither pure copper nor pure aluminium react with alumina. With the Al–2%Cu matrix wire in the as-cast condition, on the other hand, molten wire strengths are significantly lower after prestressing as compared with the homogenized matrix, see Fig. 4 and compare with Fig. 3. Fibre damage therefore accumulates during prestressing at a far higher rate than expected according to the Weibull statistics. This is most likely due to the presence of intermetallics, which are found in the as-cast condition and are essentially removed after solutionization of the Al–2%Cu matrix. If we compare the applied fibre stress with that needed to produce the same amount of damage on virgin fibres, we find that the fibres behave as if they experienced a stress amplified by a factor of about 1.21–1.25. The intermetallics adhering to the fibre surface apparently induce stress concentrations along the fibre, most likely by premature cracking. This effect has been documented for intermetallics and interfacial reaction layers in several earlier studies on the behaviour of fibre reinforced metals [33–36].

5. Conclusions

- A novel damage measurement method for fibre reinforced metals is presented. It is based on the tensile testing of a fibre reinforced metal above the matrix melting point and yields the density of broken or ending fibres within the composite.
- Use of this technique on Nextel 610™ alumina fibre reinforced Al and Al–2%Cu composite wires shows that the composite contains initial damage in the form of dead-ending fibres that result from processing. This observation and quantification of the density of such defects are in agreement with metallographic observations.
- Using the same measurement method on previously stressed composite wires it is found that: (i) the accumulation of damage prior to composite failure is mostly uncorrelated and governed by the two-param-

eter Weibull distribution of the virgin fibre strength, (ii) a brittle second phase at the fibre-matrix interface provokes premature fibre fracture such that a considerably higher amount of damage is introduced for the same load level, and (iii) the fibre strength is not per se affected by processing or copper additions to the matrix.

Acknowledgements

This work was funded by a joint EMPA/EPFL Ph.D. Thesis program, and by internal funding within EMPA in Thun and the Laboratory for Mechanical Metallurgy at EPFL. The authors would like to thank the 3M company for the donation of the composite wire used throughout this study and Dr. Colin McCullough (3M company) for many stimulating discussions.

References

[1] Maruyama B. In: Kelly A, Zweben C, editors. Comprehensive composite materials, vol. 3.27. Pergamon Press: Oxford; 2000. p. 1–23.
[2] Curtin WA. In: van der Giessen E, Wu TY, editors. Advances in applied mechanics, vol. 36. 1999. p. 163–253.
[3] Phoenix SL, Beyerlein IJ. In: Kelly A, Zweben C, editors. Comprehensive composite materials, vol. 1.19. Pergamon Press: Oxford; 2000. p. 1–81.
[4] Zok FW. In: Kelly A, Zweben C, editors. Comprehensive composite materials, vol. 3.08. Pergamon Press: Oxford; 2000. p. 1–32.
[5] Neussl E, Sahm PR, Flower HM. Adv Eng Mater 2000;2:587–92.
[6] Evans AG, Curtin WA. Scr Mater 1994;31:1757–60.
[7] Towata SI, Yamada SI. Trans Jpn Inst Met 1986;27:709–16.
[8] Pahutova M, Brezina J, Kucharova K, Sklenicka V, Langdon TG. Mater Lett 1999;39:179–83.
[9] Komenda J, Henderson PJ. In: Hansen N, Jensen DJ, Leffers T, Lilholt H, Lorentzen T, Pedersen AS, Pedersen OB, Ralph B, editors. Metal matrix composites – processing, microstructure and properties. Proc 12th Riso International Symposium on Materials Science, 1991, p. 449–54.
[10] Horkel T, Brezina J, Dlouhy A. Prakt Metallogr 1997;34:162–74.
[11] Nicholas T, Castelli MG, Gambone ML. Scr Mater 1997;36:585–92.
[12] Komai K, Minoshima K, Funato T. In: Masters JE, Gilbertson LN, editors. Fractography of modern engineering materials: composites and metals, vol. 2. ASTM STP 1203. American Society for Testing and Materials ASTM; 1993. p. 145–70.
[13] Williams Jr JH, Lee SS. J Compos Mater 1978;12:348–70.
[14] Becht J, Schwalbe HJ, Eisenblaetter J. Composites 1976;october:245–8.
[15] Awerbuch J, Bakuckas JG. In: Johnson WS editor. ASTM, ASTM STP 1032; 1989. p. 68–99.
[16] Pacheco T, Nayeb-Hashemi H, Sallam HEM. J Mater Sci 1997;32:3135–42.
[17] Pacheco T, Nayeb-Hashemi H, Sallam HEM. Mater Sci Eng 1998;A247:88–96.
[18] Chen AS, Bushby RS, Scott VD. Composites, Part A 1997;28:289–97.
[19] Xu ZR, Chawla KK, Wolfenden A, Neuman A, Liggett GM, Chawla N. Mater Sci Eng 1995;A203:75–80.
[20] Moser B, Rossoll A, Weber L, Beffort O, Mortensen A. Composites, Part A 2001;32:1067–75.
[21] Weibull W. Ingeniörsvetenskapsakademiens Handlingar 1939;151.
[22] Bunsell AR, Berger MH. J Eur Ceram Soc 2000;20:2249–60.
[23] Wilson DM, Visser LR. Composites, Part A 2001;32:1143–53.
[24] Wilson DM, Visser LR. In: Ceramic Engineering and Science Proceedings. 24th Annual Conference on Composites, Adv Mater Struct B, 23–28 Jan 2000. Cocoa Beach, FL, USA, 2000, p. 363–73.
[25] McCullough C, Mortensen A, Werner PS, Déve HE, Anderson TL. Fiber reinforced aluminum matrix composite wire. Patent, United States of America, 2001.
[26] Moser B, Rossoll A, Weber L, Beffort O, Mortensen A. J Microsc 2003;209:8–12.
[27] McCullough C. Personal communication, 2001.
[28] Mortensen A, Gungor MN, Cornie JA, Flemings MC. J Met 1986;30–35.
[29] Daniels HE. Proc R Soc 1944;A 183:405–35.
[30] Coleman BD. J Mech Phys Solids 1958;7:60–70.
[31] Mortensen A, Pedersen OB, Lilholt H. Scr Mater 1998;38:1109–15.
[32] Moser B. Deformation and fracture of continuous alumina fibre reinforced aluminium, Department of Materials Science. EPFL; 2002.
[33] Metcalfe AG. J Compos Mater 1967;1:356–65.
[34] Fukunaga H, Pan J. In: Liaw PK, Gungor MN, editors. Fundamental relationships between microstructure and mechanical properties of metal-matrix composites. 1990. p. 37–45.
[35] Ochiai S, Murakami Y. In: Kawata K, Akasaka T. editors. Composite materials. Japan–U.S. Conference on Composite Materials, Tokyo, Japan, 1981, p. 194–203.
[36] Shorshorov MK, Ustinov LM, Zirlin AM, Olefirenko VI, Vinogradov LV. J Mater Sci 1979;14:1850–61.
[37] 3M Company. Nextel Ceramic Textiles Technical Notebook (Available from: http://www.3m.com/ceramics/misc/tech_notebook.jhtml), 2002.